

25p.

X68 15752

N65-88844

Code 2 A

(NASA TMX-50 674)  
# 1

**SOME ASPECTS OF NOISE ANALYSIS OF  
INTERFEROMETER SPECTROMETERS**

Dale R. Lumb and  
Instrumentation Division

Gordon C. Angusson  
Space Sciences Division

Ames Research Center  
Moffett Field California

June 1963

7 refs Presented at the

12th International Acoustophysical Symp.,  
Liege, Belgium, June 24-26, 1963

Available to NASA Offices and  
NASA Centers Only.

## A B S T R A C T

### SOME ASPECTS OF NOISE ANALYSIS OF INTERFEROMETER SPECTROMETERS

15752

This paper analyzes the appearance and distribution of noise on a spectrum obtained by a Fourier transformation of an interferogram which was the source of the spectrum and noise.

This is accomplished through a discrete formulation by use of sampling theory and statistical methods. As a consequence of this formulation, a noise comparison of conventional spectrometers and interferometers is readily obtained which verifies that Fellgett's advantage does hold for interferometers with non-background limited detectors.

**Available to NASA Offices and  
NASA Centers Only.**

## INTRODUCTION

The purpose of this paper is to analyze the statistical characteristics of noise existing on a spectra when the spectra have been obtained by means of a two-beam interferometer spectrometer. In this analysis the distribution of noise associated with a spectrum obtained by a Fourier transform of an interferogram will be derived. Also, it will be shown that the use of an interferometer spectrometer has a  $\sqrt{M}$  signal-to-noise advantage over a conventional spectrometer when the detector used is non-background limited,  $M$  being the number of resolvable spectral components. This advantage in signal-to-noise ratio is commonly referred to as Fellgett's advantage.

## THE INTERFEROGRAM AND ITS TRANSFORM

A considerable number of papers have been written on the interferometer spectrometer; consequently, the interferometer and its basic theory will be discussed here only to the extent needed for orientation. (ref 1, 2)

Assume that an interferometer is illuminated by a monochromatic coherent source of constant intensity. Then, the interference intensity wave is  $I(t) = I(1 + \cos \gamma \omega t)$

where  $I = k^2 \cdot \frac{1}{2} \cdot \frac{c}{\lambda} \cdot \frac{1}{2} \cdot \frac{1}{2}$ ,  $\omega = 2\pi f$ ,  $f = c/\lambda$ ,  $\gamma = 2v/c$

$I$  is the light intensity,  $\lambda$  is the wavelength of light,  $c$  is the velocity of light and  $v$  is the velocity of the interferometer mirror. For heterochromatic radiation the interference wave becomes

$$I(t) = \int_0^{\infty} I(\omega) [1 + \cos \omega t] d\omega \quad (1)$$

This intensity wave is incident on a detector; thus, the output of the detector is proportional to (1) and is of the form

$$e(t) = c + \int_0^{\infty} d(\omega) \cos [\gamma \omega t + \phi(\omega)] d\omega \quad (2)$$

The right hand term of (2) is then essentially an electrical analog of the original optical electric field strength scaled down in frequency by the factor  $\gamma$ . The phase angles  $\phi(\omega)$  will be zero, provided input intensity fluctuations do not occur, all system parameters are linear, and the proper time origin is established. The desired spectrum is obtained from the Fourier transform of <sup>the</sup> non d-c term of the interferogram equation (2), and the transform may be expressed as

$$\mathcal{F}[e(t)] = E(\omega) = \int_{-\infty}^{\infty} e(t) \cos \omega t dt + j \int_{-\infty}^{\infty} e(t) \sin \omega t dt \quad (3)$$

where the first and second integrals transform the even and odd parts of  $e(t)$  respectively. In particular, if the phase angle  $\phi(\omega) = 0$  for all  $\omega$  in (3), then  $e(t)$  is an even function and the second integral in (3) is zero.

# DISCRETE FORMULATION

In general most spectra observed will be continuous. However, provided that sampling theory is correctly applied, the formulas of Fourier transformation spectroscopy may be expressed in a discrete form as well as the more familiar integral representation. For the purpose of this paper the discrete formulation has several advantages and will therefore be used in the following analysis.

Sampling Theory shows (see, for example, Reference 3) that if a function is time-limited to T seconds (i.e., the function is zero at all points outside an interval T seconds in duration) and contains negligible frequency components greater than B cycles per second, then the function (i.e. reconstructed) (and therefore its Fourier transform) may be completely determined by 2BT samples taken in the time domain at intervals of  $1/2B$  seconds\* or in the frequency domain at intervals of  $1/T$  cycles per second from -B to +B.

If sampling theory is used ~~(2)~~ then one may write Equation (1) as

$$I(t) = \sum_{i=1}^M I_i (1 + \cos \gamma \omega_i t) \quad (4)$$

where  ~~$k = 2\pi/\lambda$~~ ,  ~~$\omega_i = 2\pi f_i$~~ ,  $\omega_i = 2\pi f_i$ ,  $f_i = c/\lambda_i$ ,  $\gamma = 2\pi/c$  and

Equation (2) becomes

$$e(t) = C + \sum_{i=1}^M d_i \cos(\gamma \omega_i t + \phi_i), \quad (5)$$

\*If a frequency band from  $f_1$  to  $f_2$  is employed where  $f_1 \neq 0$ , then the minimum sampling rate may range from  $2(f_2 - f_1)$  to  $4(f_2 - f_1)$  depending on  $f_2$  and  $f_1$ . Refer to Theorem X, page 56, Reference 5.   
 samples per sec

And Equation (3) becomes

$$E(\omega_k) = \Delta t_i \sum_{i=-BT}^{BT} e\left(\frac{i}{2B}\right) \cos \omega_k t_i + j \Delta t_i \sum_{i=-BT}^{BT} e\left(\frac{i}{2B}\right) \sin \omega_k t_i \quad (6)$$

lower case  $e$

where  $\omega_k = 2\pi k/T$ ,  $k = \pm 1, \pm 2, \dots, \pm BT$ ,  $\Delta t_i = 1/2B$ ,  $t_i = i/2B$

and  $e\left(\frac{i}{2B}\right) = e(t) \Big|_{t=i/2B}$

Several observations should be made at this point with regard to the generality of (4) and (5). First, owing to physical limitations of the instrument, (4) holds only for a limited observation time  $T$ . Hence, the true detector signal is not (5) but is  $e_T(t)$ , where

$$e_T(t) = e(t) h(t) \quad \text{with} \quad h(t) = \begin{cases} 1 & -T/2 \leq t \leq T/2 \\ 0 & \text{elsewhere} \end{cases} \quad (7)$$

and  $e(t)$ , is given by (5). However, it may be shown that the Fourier transform of the truncated wave may be obtained by multiplying the real and imaginary amplitudes of the transform of  $e(t)$  for frequency  $f_1$  by

$$\left[ \frac{\sin \pi T (f - f_1)}{\pi (f - f_1)} + \frac{\sin \pi T (f + f_1)}{\pi (f + f_1)} \right]$$

instead of

$$[ \delta(f - f_1) + \delta(f + f_1) ]$$

which would be the case if  $e_T(t)$  were not time-limited. Furthermore, the amplitude components,  $d_i$ , of Equation (5) are proportional to the amplitudes of the magnitude of the Fourier transform at the sampling points  $\omega_i = 2\pi i/T$  i.e.,

$$d_i = \frac{2}{T} \left| \int [e_T(t)] \right| \omega_i = 2\pi i \quad (8)$$

where the factor  $\frac{2}{T}$  appears because equation (6) is in the form of a Fourier sin-cos series and there is a difference of a factor of  $\frac{2}{T}$  in the definition of the series coefficients and of this transform.

Secondly, the generality of representing the interference wave (4)

(1) by using a discrete sum of M terms to cover the continuum of frequencies  $f_1$  to  $f_M$  needs to be <sup>considered</sup> explained.

Essentially, the mechanism of the interference process and its detection is one of compressing and translating the spectrum of optical frequencies into a wave,  $e_T(t)$ , with a spectrum of frequencies say from 0 to B cps, which may be in the audio frequency range. This is accomplished by mapping the intensity pattern of the optical interferogram into its electrical representation  $e_T(t)$ .

The examination of a point which requires consideration then is, how good will be the representation of the desired optical spectrum <sup>be,</sup> if it is obtained from the Fourier transform of  $e_T(t)$ , which is both time-limited (T sec.), approximately band-limited (B cps) and represented by a discrete number of independent terms. The answer to this question will be given later in this paper, where it is shown that the number of resolvable components M, required to represent the true optical spectrum of a continuum of frequencies  $f_1$  to  $f_M$  is BT. Since the signal  $e_T(t)$  may be completely

represented by 2BT independent data, according to sampling theory, the summations of (4) and (5) completely describe the desired optical spectrum within the resolution determined by  $e_T(t)$  when the source under observation consists of a continuum of frequencies. It should be noted that BT independent amplitude data and BT independent phase data are required to completely specify  $e_T(t)$ , but the phase information is deleted in the computation of the ~~magnitude~~ <sup>magnitude</sup> of the Fourier transform.

#### TRANSFORMATION OF ADDITIVE NORMAL INTERFEROGRAM NOISE

As indicated in the previous section, an interferogram is a time record whose Fourier transform gives the spectral data of the observed source. Any noise in the time record is redistributed when the Fourier transformation is performed. There has been some confusion as to how such a transformation <sup>a</sup> affects the noise in the spectrum, as compared with a conventional spectrometer. In the following section it will be shown that, although the noise is redistributed in a different form with different statistical parameters, the signal-to-noise ratio per spectral element of a spectrum derived from an interferogram does exhibit Fellgett's advantage.

To determine the effect on the spectrum of noise appearing on the time function, first consider the noise probability density function and how it transforms. In doing this, it will be necessary to assume that the process does not introduce additional noise power. This assumption is reasonable in practice, since the discrete formulation is possible by sampling theory, thus allowing the operation to be performed by a digital computer program.



Due to detector noise (ref. 4, 5) every amplitude sample of the interferogram  $e_T(t)$  will be measured with some uncertainty, say  $\epsilon_1$  for the  $i^{\text{th}}$  sample. Then the resultant interferogram will be

$$e_T(t) = e_T'(t) + \epsilon_T(t) \quad (9)$$

where  $e_T'(t)$  is the true signal and  $\epsilon(t)$  is the noise, or in a sampled form

$$e_i = e_i' + \epsilon_i, \quad i = \pm 1, \pm 2, \dots, \pm BT \quad (10)$$

Assume that the random noise  $\epsilon_T(t)$  belongs to a normal probability distribution with zero mean. This statistical characterization will include all random normally distributed noise that is additively superimposed on the true interferogram.

The probability density function for any error  $\epsilon_1$  is given by

$$P(\epsilon) d\epsilon = \frac{1}{(2\pi\sigma^2)^{1/2}} \exp \left\{ -\frac{\epsilon^2}{2\sigma^2} \right\} d\epsilon \quad (11)$$

where  $\sigma^2$  = variance of  $\epsilon_i$ . It can be verified that the variance,  $\sigma^2$  is equal to the average power of the amplitudes of  $\epsilon(t)$ . Thus, equation (11) expresses the statistics of the time domain noise,  $\epsilon(t)$  on the interferogram  $e_T(t)$ . Now that the time domain noise to be considered has been formulated, the goal will be to statistically characterize this noise in the transformed spectrum.

$\epsilon_T(t)$  expressed in terms of its sample form may be transformed by (6) and is

$$\epsilon(\omega) = \alpha(\omega) + j\beta(\omega)$$

where

$$\alpha(\omega) = \frac{1}{2B} \sum_{n=-BT}^{BT} \epsilon_T\left(\frac{n}{2B}\right) \cos\left(\frac{n\omega}{2B}\right) \quad (12)$$

and

$$\beta(\omega) = \frac{1}{2B} \sum_{n=-BT}^{BT} \epsilon_T\left(\frac{n}{2B}\right) \sin\left(\frac{n\omega}{2B}\right)$$

For a given frequency  $\epsilon(\omega)$  is a weighted sum of all the  $\epsilon_i$  so that by the use of the central limit theorem (reference 6) it can be shown for large BT that the random variables  $\alpha$  and  $\beta$  are independent and the probability distributions of the amplitudes of  $\alpha(\omega)$  and  $\beta(\omega)$  are represented by

$$P(\alpha) = \frac{1}{(\rho^2\pi)^{1/2}} \exp\left\{-\frac{\alpha^2}{\rho^2}\right\} d\alpha$$

and

$$P(\beta) = \frac{1}{(\rho^2\pi)^{1/2}} \exp\left\{-\frac{\beta^2}{\rho^2}\right\} d\beta \quad (13)$$

where

$$\rho^2 = \langle 2\alpha^2 \rangle = \langle 2\beta^2 \rangle = \langle |\epsilon(\omega_k)|^2 \rangle$$

Since  $\epsilon_T(t)$  was assumed to be random noise, the  $\epsilon_i$  are statistically independent and consequently  $\rho^2$  is not a function of frequency. The relation between the variance of the time samples and the variance of the frequency samples is given by (reference <sup>6</sup>2)

$$\rho^2 = \frac{T}{2B} \langle |\epsilon_T(\frac{1}{2B})|^2 \rangle = \frac{T}{2B} \sigma^2 \quad (14)$$

Furthermore, the joint distribution of  $\alpha$  and  $\beta$  is the bi-variate normal distribution

$$P(\alpha, \beta) \cdot d\alpha d\beta = \frac{1}{\rho^2 \pi} \exp \left\{ -\frac{\alpha^2 + \beta^2}{\rho^2} \right\} d\alpha d\beta \quad (15)$$

These expressions describe the statistical behavior of noise alone irrespective of the true signal, but these formulations readily permit the characterization of the transformed noise superimposed on the true spectrum.

From (9) the Fourier transform of the received time record  $e_T(t)$  is

$$\mathcal{F}[e_T(t)] = \mathcal{F}[e'_T(t)] + \mathcal{F}[\epsilon_T(t)] \quad (16)$$

or

$$E(\omega) = E'(\omega) + \epsilon(\omega)$$

where

$$E'(\omega) = a(\omega) + j b(\omega)$$

and

$$\epsilon(\omega) = \alpha(\omega) + j \beta(\omega)$$

From (8) and (16) the spectrum of intensity as a function of frequency becomes for the general case

$$\left| \frac{2E(\omega)}{T} \right| = \frac{2}{T} \left| [a(\omega) + \alpha(\omega)] + j[b(\omega) + \beta(\omega)] \right| \quad (17)$$

The probability distribution of the variable  $\left| \frac{2E(\omega)}{T} \right|$ , where the transform of the noise is described according to (15) will be representative of the way the noise is distributed over the spectrum.

For each sample,  $a(\omega_k)$  and  $b(\omega_k)$  are fixed, and  $\left| \frac{2E(\omega)}{T} \right|$  can therefore be considered by means of the variables

$$\begin{aligned} x &= \frac{2}{T} (a + \alpha) \\ y &= \frac{2}{T} (b + \beta) \end{aligned}$$

From (15)  $P(x, y) dx dy = \frac{1}{2\pi\psi^2} \exp \left\{ -\frac{1}{2\psi^2} \left[ \left(x - \frac{2a}{T}\right)^2 + \left(y - \frac{2b}{T}\right)^2 \right] \right\} dx dy$

where

$$\psi^2 = \left\langle \left( \frac{2\alpha}{T} \right)^2 \right\rangle = \frac{2\sigma^2}{T^2}$$

Therefore, from (14)

$$\psi^2 = \frac{\sigma^2}{BT} \quad (18)$$

With the change of variables  $r = (x^2 + y^2)^{1/2} = \left| \frac{2E(\omega)}{T} \right|$ ,  $\theta = \tan^{-1} y/x$

then  $dy dx = r dr d\theta$

and 
$$\begin{aligned} \int_{-\infty}^{\infty} \int_{-\infty}^{\infty} P(x, y) dx dy &= \int_0^{\infty} \int_0^{2\pi} r P(r, \theta) dr d\theta \\ &= \int_0^{\infty} \int_0^{2\pi} \frac{r}{2\pi\psi^2} \exp \left\{ -\frac{1}{2\psi^2} \left[ r^2 + \left(\frac{2a}{T}\right)^2 + \left(\frac{2b}{T}\right)^2 - \frac{4ar}{T} \cos \theta - \frac{4br}{T} \sin \theta \right] \right\} dr d\theta \\ &= \int_0^{\infty} \frac{r}{\psi^2} \exp \left\{ -\frac{1}{2\psi^2} (r^2 + \mu^2) \right\} I_0 \left( \frac{r\mu}{\psi^2} \right) dr \end{aligned} \quad (19)$$

where

$$\mu = \frac{2}{T} (a^2 + b^2)^{1/2}$$

Therefore, the desired distribution of  $r = \left| \frac{2E(\omega)}{T} \right|$  is

$$P(r) dr = \frac{r}{\psi^2} \exp \left\{ -\frac{1}{2\psi^2} (r^2 + \nu^2) \right\} I_0 \left( \frac{\nu r}{\psi^2} \right) dr \quad (20)$$

where  $I_0(z) = \sum_{m=0}^{\infty} \left( \frac{z}{2} \right)^{2m} / (m!)^2$  is the zero-order Hyperbolic Bessel function. An alternate form of  $I_0(z)$ , useful for large values of the argument, is

$$I_0(z) = \frac{e^z}{(2\pi z)^{1/2}} \left( 1 + \frac{1}{8z} + \frac{9}{128z^2} + \dots \right) \quad (21)$$

The properties of the density function (20) may be described by its moments which are given by

$$\langle r^n \rangle = (2\psi^2)^{n/2} \Gamma\left(\frac{n}{2} + 1\right) \exp\left\{ -\frac{\nu^2}{2\psi^2} \right\} M\left(\frac{n}{2} + 1; 1; \frac{\nu^2}{2\psi^2}\right) \quad (22)$$

(Reference <sup>7</sup>) where  $M$  is a confluent hypergeometric function.

In particular,

$$\langle r^2 \rangle = \nu^2 + 2\psi^2 \quad (23)$$

and for no signal present (only noise)

$$\langle r \rangle = \psi \left( \frac{\pi}{2} \right)^{1/2} \quad (24)$$

and

$$\langle r^2 \rangle = 2\psi^2.$$

The expression (20) represents the probability distribution of the amplitudes of the spectra which includes the true spectrum and the superimposed noise. The particular shape of the distribution for any amplitude

(any sample in the frequency domain) is dependent upon the magnitude of the true signal. That is,

$$\mu = \frac{2}{T} \left\{ [a(\omega)]^2 + [b(\omega)]^2 \right\}^{1/2} \quad (25)$$

Figure 1 shows in normalized form  $\psi P(r)$  vs.  $r/\psi$  for several values of  $\mu/\psi$ .

For purpose of interpretation (20) can be closely approximated in two particular cases: First for  $\mu = 0$  and for small  $\mu$  over the range of  $r \ll \psi$ , then  $I_0\left(\frac{r\mu}{\psi^2}\right) \approx 1$

and

$$P(r) dr \approx \frac{r}{\psi^2} \exp \left\{ -\frac{r^2}{2\psi^2} \right\} dr \quad (26)$$

This is the Rayleigh distribution presented in normalized form in Figure 1 with  $\mu/\psi = 0$ . The significant point is that the distribution for zero signal is not centered about zero. In fact the peak for the Rayleigh distribution occurs at  $r = \psi$ . The first and second moments are given by (24) as is shown in Figure 1 by the curve for  $\mu/\psi = 0$ .

Consider the second case where the amplitude of the true spectrum is large compared to  $\psi$ , i.e.,  $\mu \gg \psi$ . For large  $z$  from the series form of (21)  $I_0(z) \approx e^z / (2\pi z)^{1/2}$ , so that

$$\begin{aligned} (20) \text{ can be approximated by } \\ p(r) dr \approx \frac{r}{\psi^2} \exp \left\{ -\frac{1}{2\psi^2} (r^2 + \mu^2) \right\} \cdot \frac{\exp \left\{ \frac{r\mu}{\psi^2} \right\}}{(2\pi \frac{\mu}{\psi^2})^{1/2}} dr \\ = \frac{1}{(2\pi \psi^2)^{1/2}} \left( \frac{r}{\psi} \right)^{1/2} \exp \left\{ -\frac{1}{2\psi^2} (r - \mu)^2 \right\} dr \quad (27) \end{aligned}$$

which further closely approximates a normal distribution

$$p(r) dr \approx \frac{1}{(2\pi \psi^2)^{1/2}} \exp \left\{ -\frac{1}{2\psi^2} (r - \mu)^2 \right\} dr$$

## NOISE COMPARISON

Equation (20) and its approximation (27) characterize the statistics of the transform of the interferogram which includes signal plus normal (Gaussian) noise. Now a comparison of interferometers and conventional spectrometers with respect to errors caused by normal (Gaussian) noise can be made. The only noise which will be considered is that which originates in the detector.

Detector noise is generally ascribed to two sources; that which is intrinsic in the detector itself and that which is generated in the detector by the statistical fluctuations of the incident photons. Detectors whose intrinsic noise is less than that due to incident photon fluctuation are known either as photon limited or background limited detectors. In the case of the conventional spectrometer the signal to noise ratio is not a function of the source of the detector noise. This is not the case however, for the interferometer spectrometer. If the interferometer detector is background-limited the detector sees simultaneously, the total radiation from all of the spectral elements while the detector of the conventional spectrometer is affected only by the radiation from one spectral element. Thus, the interferometer detector noise is  $M$  times greater. Only the non-background-limited detectors will be considered at this time, with the background-limited detectors being treated later. The former class of detectors is both large and important, being as all detectors used in the infrared spectral region are considered to be non-background limited.

To compare the noise errors of a conventional and interferometer spectrometer it is necessary to assume the same scan time,  $T$ , for the conventional spectrometer as for the interferometer and the same number of resolved spectral elements,  $M = BT$ . Then the time allowed for the

measurement of each resolved spectral element is  $1/B$  and the required bandpass is approximately  $B$  cycles per second. <sup>Therefore,</sup> Thus, the noise can be limited to a bandwidth of  $B$  and the probability distribution of the noise is characterized by the same  $\sigma^2$  as used in equation (11). Thus, the amplitude error per spectral element for the conventional case obeys the statistics expressed by (11). Also, one may write in an analogous manner to (10)  $S_1 = S_1' + \epsilon_1$  where  $S_1'$  is the true signal amplitude and  $\epsilon_1$  is the superimposed noise error. Hence, for <sup>the</sup> statistical representation <sup>of</sup> for each sample (amplitude)  $S_1$ , the true signal  $S_1' = \mu_1$  is fixed and can be considered as the mean, so that the probability density function of the amplitudes is

$$P(S) dS = \frac{1}{(2\pi\sigma^2)^{1/2}} \exp\left\{-\frac{1}{2\sigma^2}(S-\mu)^2\right\} dS \quad (29)$$

By way of comparison of amplitude errors for the interferometer spectrometer and the conventional spectrometers, note the results (20) and (29).



and in particular (28) and (29) for large signal values. The variance indicates the spread of the distribution and the smaller the variance the more peaked the distribution becomes. From (18)

$$\psi^2 = \left(\frac{1}{BT}\right) \sigma^2$$

Hence it can be concluded that the amplitude noise error per spectral element for the interferometer belongs, with a given probability, to a smaller amplitude range. That is, the time domain amplitude errors are redistributed into amplitude errors in the frequency domain where the most probable amplitude range has been decreased. This is illustrated in Figure 2, where arbitrarily  $BT$  was chosen to be 100. Later it will be shown that  $BT$  is the number of resolvable components in the spectrum.

On the basis of these results, the noise power per spectral element for the conventional spectrometers and the interferometer can be computed and compared. Any computed spectral amplitude is of the form

$$r = \frac{2}{T} \left| \int [e_r(t)] \right|$$

and the corresponding true amplitude is  $\mu = \frac{2}{T} (a^2 + b^2)^{1/2}$

The mean square error  $\langle (r - \mu)^2 \rangle$  is then the average noise power,

$N_I^2$ , which may be expressed as

$$N_I^2 = \langle (r - \mu)^2 \rangle = \langle r^2 \rangle - 2 \langle r \rangle \mu + \mu^2$$

using equation (23),

$$N_I^2 = 2\psi^2 + 2\mu(\mu - \langle r \rangle) \quad (30)$$

The mean of  $r$ ,  $\langle r \rangle$ , has been computed from <sup>22</sup>(23) and  $N_I^2$  evaluated as a function of true signal,  $\mu$ . The results are plotted in Figure 3. It is seen that the noise power is a function of the signal and that the maximum noise power,  $N_{I \text{ max}}$ , occurs at  $\mu = 0$  and in terms of variance

$$N_{I \text{ max}} = 2\psi^2$$

The minimum noise power occurs where  $\mu/\psi = 1$ , in which case

$$N_{I \text{ min}} = .87\psi^2$$

Furthermore, for larger  $\mu/\psi$ ,  $N_I$  quickly approaches  $\psi^2$  or <sup>8</sup>relating  $\psi^2$  to the variance (or average noise power) of the time amplitude noise by <sup>8</sup>(23) gives

$$N_I^2 = \frac{\sigma^2}{BT}$$

31  
(20)

In the time record the amplitude noise power was  $\sigma^2$ . Since the same additive noise occurs directly on the spectrum of the conventional case, then  $\sigma^2$  is the average noise power per spectral element assuming the same scan time  $T$  and bandwidth  $B$  in both cases.

It is desired now to prove that  $BT$  is equal to  $M$ , where  $M$  is the number of spectral components that an interferometer is able to resolve. Suppose that a source emits energy of two frequencies  $f_1$  and  $f_2$ . The interferometer produces an output whose Fourier transform is of the form

$$\mathcal{F}[e_T(t)] = \frac{I_1 d_1}{2} \frac{\sin \pi T(f - f_1)}{\pi T(f - f_1)} + \frac{I_2 d_2}{2} \frac{\sin \pi T(f - f_2)}{\pi T(f - f_2)}$$

(showing only the positive frequency terms  
(neglecting negative frequencies)). According to the Rayleigh criterion,

the two spectral lines are independent and resolvable when the maximum

of one coincides with a first zero of the other. In the above example, then, the frequencies  $f_1$  and  $f_2$  are resolvable if

$\delta f = |f_1 - f_2| = \frac{1}{T}$ . If the spectral range of the source is from  $f_a$  to  $f_b$  and the resolution is  $\delta f$ , then the number of distinguishable independent spectral elements is  $M = \frac{f_b - f_a}{\delta f}$ .

In the frequency mapping of the interferometer  $f_b - f_a = B$  and  $\delta f = \frac{1}{T}$  so that  $M = BT$ . Thus, from (29) the noise voltage for an interferometer is

$$N_I = \frac{\sigma}{\sqrt{M}} \quad (32)$$

From this it may be seen that the noise voltage of an interferometer is  $1/\sqrt{M}$  times the noise voltage for a spectrometer. Since the signal levels are the same for both, this results in a  $\sqrt{M}$  signal-to-noise advantage for the interferometer, which has been called Fellgett's advantage. This advantage holds for non-background limited detectors. If the detector is background limited then the mean rate of photons  $\langle I_r \rangle$  incident on the detector and therefore the noise power is  $M$  times as great for the interferometer as for the conventional spectrometer. Thus, (32) for interferometer noise voltage becomes  $N_I = \sigma$  and Fellgett's advantage is cancelled.

## SUMMARY

The probability distributions which govern the noise superimposed on the signal for both the interferometer and conventional spectrometer are derived and compared. For interferometers, the variance, and hence the spread of error amplitudes per spectral element, is less than for the same time observation and same resolution for the conventional case. Furthermore, the noise power in the spectrum is shown to be dependent on the signal, and varies from  $\frac{2\sigma^2}{M}$  to approximately  $\frac{\sigma^2}{M}$  and hence the signal-to-noise voltage ratio comparisons show an advantage of from  $\sqrt{M/2}$  to approximately  $\sqrt{M}$  for the interferometer.

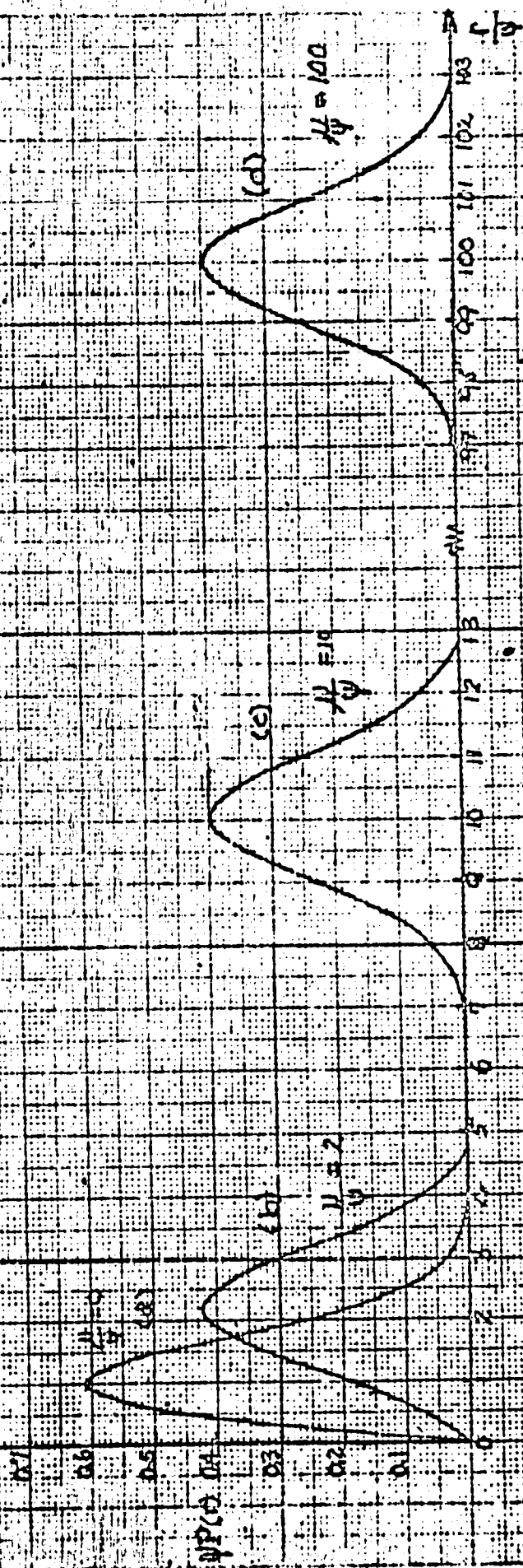


Fig. 1 Normalized probability distribution curves of the amplitude of interferometer spectra which includes the true spectrum and the superimposed noise for different values of the true signal  $U/\psi$ . This demonstrates the dependence of the distribution of the amplitude of the true signal. Note: For zero signal, the distribution (Rayleigh) is centered at  $r = \psi$ .

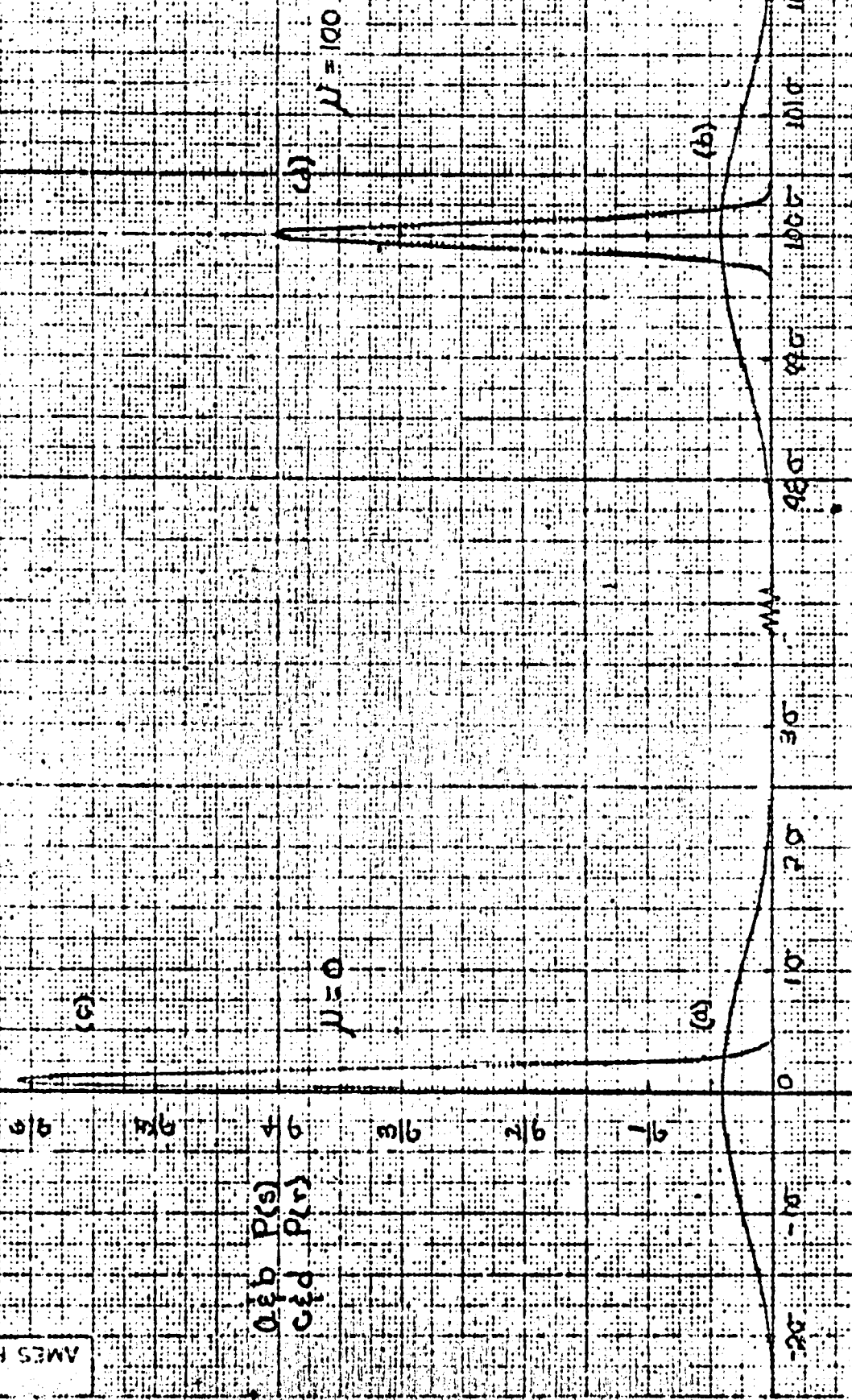


Fig. 2 Comparison of noise distribution curves for conventional and interferometer spectrometers.

Curves a and b are for a conventional spectrometer with  $P(S)$  plotted against  $S$ , a variance of  $\sigma^2$  and  $\mu = 0$  and 100 respectively. Curves c and d are for an interferometer spectrometer with  $P(r)$  plotted against  $r$ , a variance of  $\sigma^2$  and  $\mu = 0$  and 100.

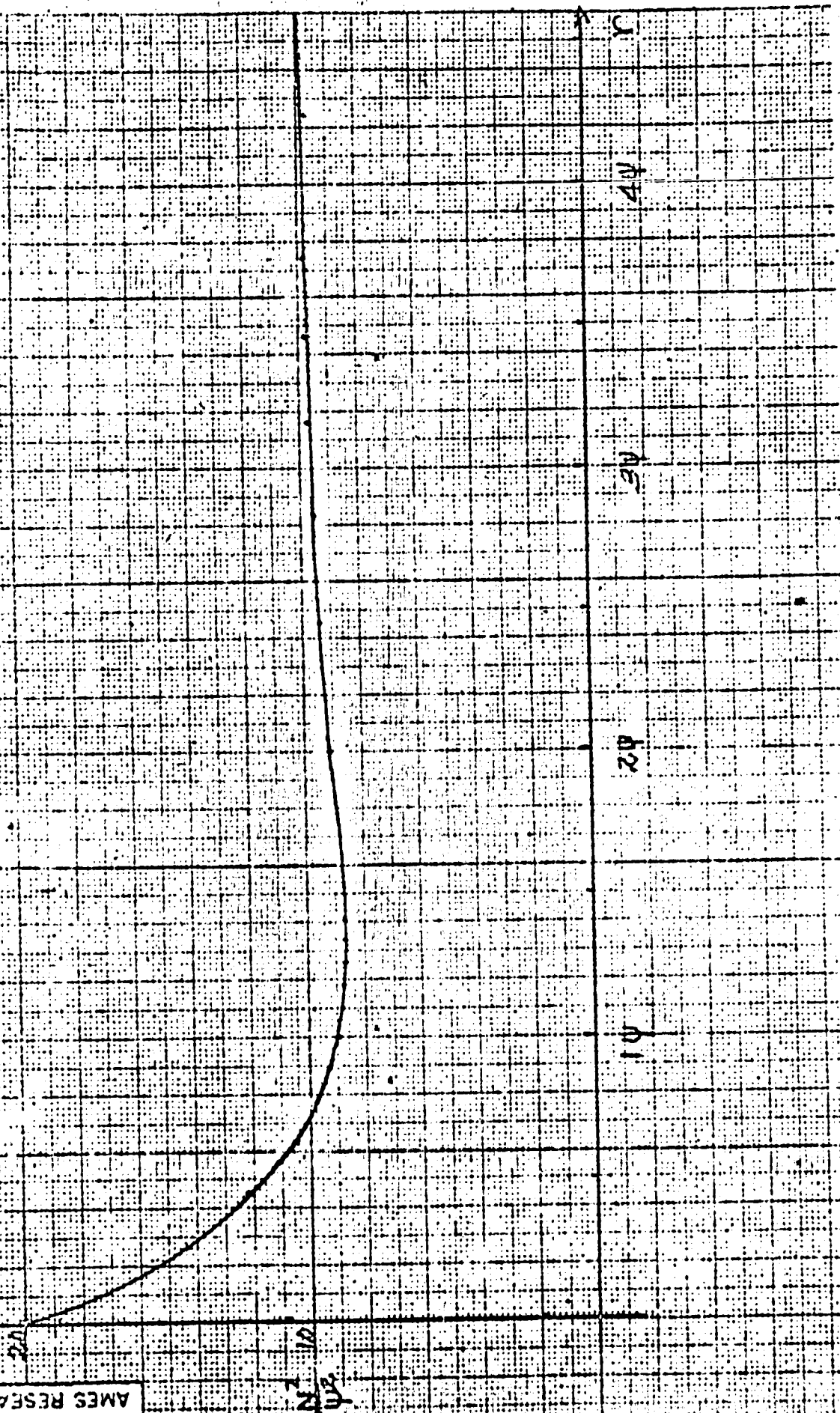


Fig. 3 Noise power curve showing the dependence of noise power on the total signal.

## REFERENCES and BIBLIOGRAPHY

1. Connes, J., Revue d'Optique, February (1962), No. 2, (4 articles).
2. Strong, John H., "Concepts of Classical Optics", Appendix F, W. H. Freeman and Company, San Francisco, Calif. (1958).
4. Holter, M. R., Nudelman, Sol, and others, "Fundamentals of Infrared Technology", The MacMillan Company, New York (1962).
5. Petritz, R. L., "Photoconductivity Conference", Pages 49-77, John Wiley & Sons, Inc., New York, (1956).
3. Black, H. S., "Modulation Theory," Van Nostrand Co., Inc., N.Y. (1953).
6. Goldman, Stanford, "Information Theory", Pages 114-116, Prentice-Hall, Inc., N.Y. (1953).
7. Rice, S.O. Bell System Tech. Jour., <sup>Page</sup> 24, 101, (1945).



### **Acknowledgement**

The authors wish to acknowledge the helpful suggestions and criticisms which they received from Mr. James A. White, Chief of the Instrumentation Division of Ames Research Center.